AUTOMATIC GENERATION OF DIGITAL BUILDING MODELS FOR COMPLEX STRUCTURES FROM LIDAR DATA

Changjae Kim [a], Ayman Habib [a, *], Yu-Chuan Chang [a]

[a]Geomatics Engineering, University of Calgary, Canada - habib@geomatics.ucalgary.ca, (cjkim, ycchang)@ucalgary.ca

Commission IV, WG IV/3

KEY WORDS: LiDAR, Ground/non-ground Separation, Building Hypotheses, Segmentation, Digital Building Model

ABSTRACT:

Automated and reliable 3D reconstruction of man-made structures is important for various applications in virtual reality, city modeling, military training, etc. This paper is concerned with the automated generation of Digital Building Models (DBM) associated with complex structures comprised of small parts with different slopes, sizes, and shapes, from a LiDAR point cloud. The proposed methodology consists of a sequence of four steps: ground/non-ground point separation; building hypothesis generation; segmentation of planar patches and intermediate boundary generation; and boundary refinement and 3D wire frame generation. First, a novel ground/non-ground point classification technique is proposed based on the visibility analysis among ground and non-ground points in a synthesized perspective view. Once the LiDAR point cloud has been classified into ground and non-ground points, the non-ground points are analyzed and used to generate hypotheses of building instances based on the point attributes and the spatial relationships among the points. The third step of the proposed methodology segments each building hypothesis into a group of planar patches while simultaneously considering the attribute similarity and the spatial proximity among the points. The intermediate boundaries for segmented clusters are produced by using a modified convex hull algorithm. These boundaries are used as initial approximations of the planar surfaces comprising the building model of a given hypothesis. The last step of the proposed methodology utilizes these initial boundaries to come up with a refined set of boundaries, which are connected to produce a wire frame representing the DBM. The performance of the proposed methodology has been evaluated using experimental results from real data.

1. INTRODUCTION

Recent developments in positioning and navigation technology is having a positive impact on the widespread adoption of LiDAR (Light Detection And Ranging) systems, leading to an abundant availability of accurate surfaces with high point density. Abstracting the huge number of points in a typical LiDAR survey and relating them to physical objects, especially man-made structures, are among the key problems being addressed by current research. Therefore, there has been significant interest in developing DBM generation methodologies for representing artificial structures in a simple way, instead of using the enormous amount of points present in the LiDAR point cloud. Various methods have been suggested for building extraction from LiDAR points. Haala et al. (1998), Brenner and Haala (1998), Vosselman and Dijkman (2001) made use of ground plan data. Several attempts based on using Digital Surface Models (DSM) and Digital Terrain Models (DTM) have been made by Brunn and Weidner (1997), Ameri (2000), and Rottensteiner and Briese (2002). This paper discusses the topic of automated generation of DBM associated with complex mad-made structures from a raw LiDAR point cloud. More specifically, we will present a new framework for DBM generation from LiDAR data, which overcomes shortcomings of existing techniques. The proposed methodology consists of four basic steps: 1) Ground/non-ground point separation; 2) Building hypothesis generation; 3) Segmentation of planar patches and intermediate boundary generation; and 4) Boundary refinement and 3D wire frame generation. First, a novel ground/non-ground point classification technique is proposed based on the visibility analysis among ground and non-ground points in a synthesized perspective view. After the original LiDAR points have been classified into ground and non-ground points, further investigation into the non-ground points is performed, to generate hypotheses of building instances. The generated hypotheses are based on the planarity and the proximity of the non-ground points. The points representing a single hypothesis might be comprised of several connected planes with different slopes and aspects. Therefore, the third step of the proposed methodology segments each building hypothesis into a group of planar patches. The proposed segmentation technique in this paper uses a voting scheme that keeps track of the point attributes. The clustering of the points is implemented based on simultaneous consideration of the attribute similarity and spatial neighborhood among the points, to provide a robust and accurate solution. Moreover, this procedure is more efficient compared to the existing methods in terms of computation load. Once the clusters are provided from the segmentation procedure, the boundary for each of the segmented clusters is derived using a modified convex hull algorithm. These boundaries will be used as initial approximations of the planar surfaces comprising the building model of a given hypothesis. The last step of the proposed methodology utilizes these initial boundaries to come up with a delineated set of boundaries which are connected to produce a wire frame representation of the DBM. Various geometric characteristics such as intersection, proximity, 2D collinearity, and height frequency are utilized to regularize initial boundaries. The detailed explanation of the proposed methodology is presented in section 2. The performance of the

* Corresponding author.

methodology is discussed in section 3. Then, concluding remarks are mentioned in section 4.

2. METHODOLOGY

As abovementioned the proposed methodology consists of a sequence of four steps: ground/non-ground point separation; building hypothesis generation; segmentation of planar patches and intermediate boundary generation; and boundary refinement and 3D wire frame generation. In this section, detailed explanation and experimental results are presented for each step.

2.1 Ground/non-ground Point Separation

The developed methodology for ground/non-ground separation is based on the assumption that non-ground points cause occlusions under perspective projection. In a perspective projection, the top and bottom of a structure are projected as two different points. These points are spatially separated by a distance referred to as the relief displacement. This displacement takes place along a radial direction from the image space nadir point, and is the cause of occlusions in perspective imagery. In this work, the presence of occlusions is detected by sequentially checking the off-nadir angles of the lines of sight connecting the perspective center and the DSM points, along the radial direction starting from the object space nadir point (Habib et al., 2007). Several synthesized perspective centers with heights close to the maximum elevation of the entire study area are introduced to more thoroughly detect the points causing occlusions. Figure 1 illustrates the basic concept of detecting non-ground points along a profile using a synthesized perspective center. By scanning for occlusions from different radial directions with multiple synthesized perspective centers, ground points are well-identified from the DSM. The DSM used in the analysis is generated by resampling the irregular LiDAR point cloud to a regular grid, using the nearest neighbor method to increase computational speed. After removing the effects caused by the roughness of the terrain, the non-ground points and ground points can be separated from one another. For more detailed explanation and experimental verification of this novel ground/non-ground point classification technique, please refer to [Habib et al., 2008].

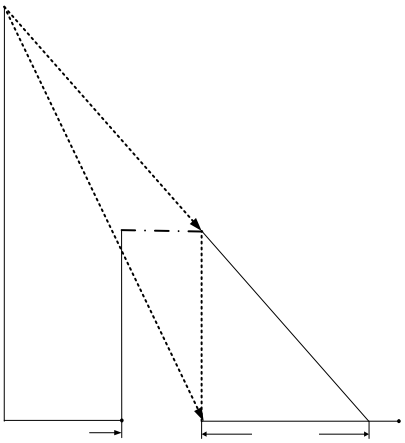

Figure 1. Basic concept of detecting non-ground points.

In this paper, raw LiDAR point data over University of Calgary, Canada, is introduced. The study area includes building structures which are connected with other complex buildings. Figure 2 and 3 shows aerial photos and the LiDAR point cloud over the area of interest, respectively.

Figure 2. Aerial photo over the area of interest.

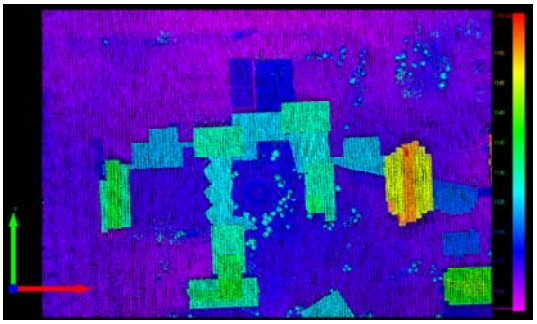

Figure 3. LiDAR points over the area of interest (colors are assigned according to their elevations).

The ground/non-ground separation algorithm is applied to the LiDAR points over the area of interest. Figure 4 shows the points which are classified into ground and non-ground points. The points in blue and red indicate ground and non-ground points, respectively.

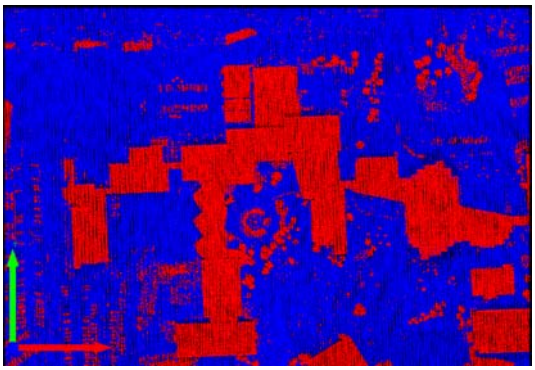

Figure 4. Separated ground and non-ground points.

2.2 Building Hypothesis Generation

Once the LiDAR point cloud has been classified into ground and non-ground points, non-ground points are further analyzed

to derive hypotheses of building instances. The generated hypotheses are based on several point attributes as well as the spatial relationships among the non-ground points. More specifically, non-ground points are classified into points pertaining to planar or rough surfaces. Using an adaptive local neighborhood for each point, one can decide whether this neighborhood defines a planar surface or not. Then, a grouping technique is applied to collect neighboring points that belong to planar surfaces while considering proximity of them in 3D space. Finally, the derived groups are filtered to generate building hypotheses based on the size of the group and their height above the terrain. The generated hypotheses are based on the prior knowledge that buildings are usually large in size with a certain minimum height above the ground. Figure 5 shows the building hypotheses generated through these procedures. In the figure, the points with different colours belong to the different building hypotheses. One should note that the points belonging to the different hypotheses might be shown in the same color due to the limitation of the number of utilized colors. In addition, a single hypothesis might consist of points from several planes. This situation happens when a structure is formed by a series of connected planes with different slopes and aspects.

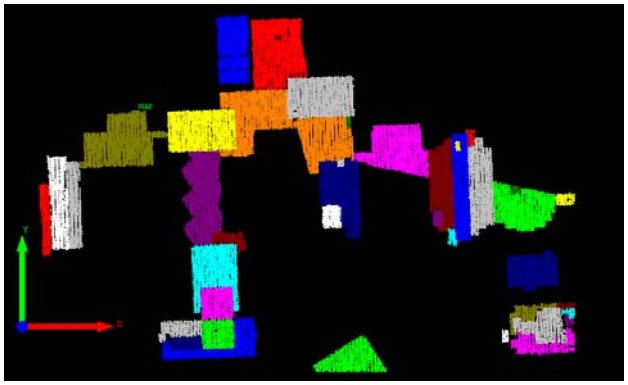

Figure 5. Generated building hypotheses.

2.3 Segmentation of Planar Patches and Intermediate Boundary Generation

The following procedure segments the points that are in a single building hypothesis, but may come from physically different planes, into a group of planar patches. The proposed segmentation technique in this paper is a voting scheme that keeps track of the point attributes, as defined by an adaptive local plane through its neighboring points, in an accumulator array. More specifically, the procedure is composed of three sub-steps: neighborhood definition; attribute derivation; and clustering of neighboring points with similar attributes. First, a neighborhood definition which considers both the three-dimensional relationships between LiDAR points and the physical shapes of surfaces is introduced and employed (Filin and Pfeifer, 2006). The physical shapes of the surfaces on which associated points are located are incorporated into the neighborhood definition. This means that points located on the same surface are considered to be possible neighbors, while taking into account the proximity of the points. Points on different surfaces, on the other hand, are not considered to be neighbors, even if they are spatially close. This definition increases the homogeneity among neighbors. Neighbors are determined using a cylinder whose axis direction changes according to the physical shape of the object in question. It is for this reason that this neighborhood definition is referred to as the adaptive cylindrical neighborhood definition. In this research, point attributes are computed based on the neighboring points identified using the adaptive cylinder method. More specifically, each point has two attributes. These attributes are the normal distances between the local plane (which is defined by neighboring points through an adaptive cylindrical neighborhood definition) and two pre-defined points, shown as origin 1 and origin 2 in Figure 6. In addition, the figure illustrates the basic concept of point attributes computation.

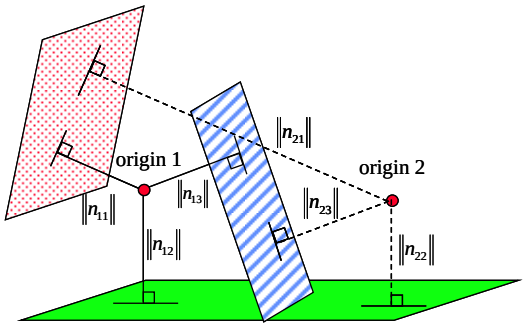

Figure 6. Basic concept of point attributes computation.

Once the attributes for all the points are computed, they are stored in an accumulator array that keeps track of the frequency of such attributes. As might be expected, points with similar attributes will lead to peaks in the accumulator array. Figure 7 and 8 shows the examples of the scanned LiDAR points and the produced accumulator array using their attributes, respectively. The LiDAR points in this area represent a gable roof, which consists of two planes with different slopes. The computed attributes from these points are voted in the accumulator array. Two groups of similar attributes, produced from the points on two different roof planes, construct two high peaks in the array.

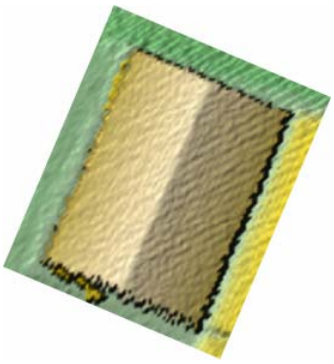

Figure 7. Scanned LiDAR points from the area including a gable roof.

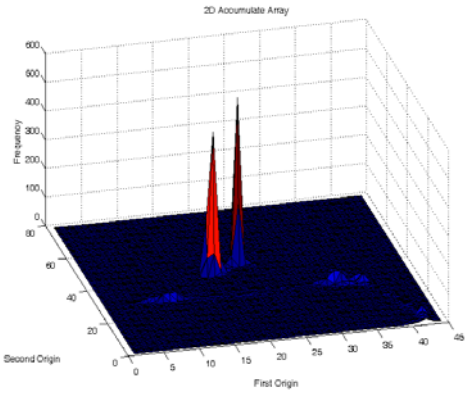

Figure 8. The produced accumulator array using the LiDAR points in Figure 7.

Points contributing to the peaks are clustered while simultaneously considering their attribute similarity and the spatial neighbourhood among the points. In other words, the clustering procedure is implemented while globally assessing the attributes in the parameter space together with the local proximity of the points in the object space at the same time. This procedure provides a robust and accurate segmentation solution. Moreover, it is more efficient compared to the existing methods in terms of computation load due to the utilization of only two attributes in the procedure. Figure 9 displays the segmentation results produced from the LiDAR point cloud in Figure 7. In the Figure 9, the points in green and blue are clustered and recorded from two highest peaks in the accumulator array in Figure 8.

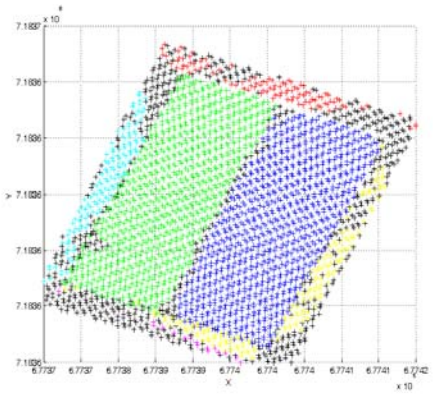

Figure 9. The produced segmentation results from the LiDAR points in Figure 7.

Figure 10 displays the results produced from the segmentation procedure applied to the generated building hypotheses in Figure 5. As before, the points in different colors belong to the different planar patches. One can compare these segmentation results, in particular those enclosed by the white solid ellipses, with the building hypothesis results in Figure 5. The points belong to a single building hypothesis have been separated into different clusters. As an additional output from the segmentation procedure, we use a least squares adjustment to derive an estimate of the plane of best fit through each cluster.

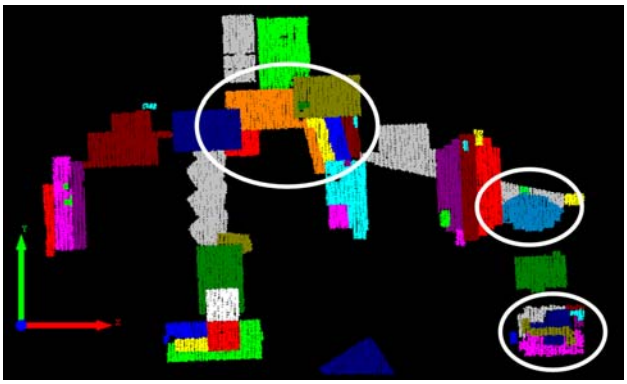

Figure 10. Clusters produced from the segmentation procedure.

The modified convex hull approach (Jarvis, 1977) is adopted to determine the boundary for each of the segmented clusters. The produced intermediate boundaries are displayed in Figure 11.

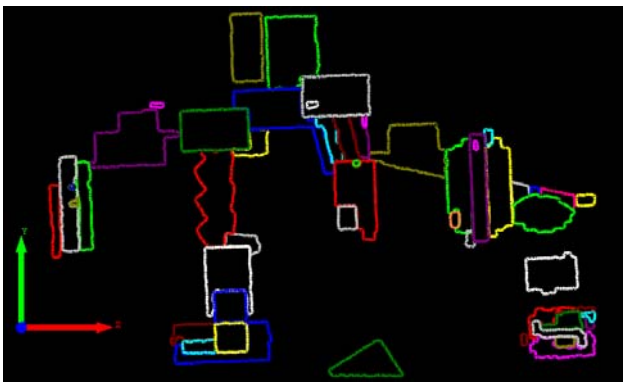

Figure 11. Intermediate boundaries produced by using the modified convex hull algorithm.

These boundaries will be used as initial approximations of the planar surfaces comprising the building model of a given hypothesis.

2.4 Boundary Refinement and 3D Wire Frame Generation

The last step of the proposed methodology utilizes the initial boundaries to come up with a refined set of boundaries, which are connected to produce a wire frame representing the DBM. The refinement process is based on several steps. The first one inspects the boundaries of the segmented patches to detect the presence of neighbouring planar patches which can be intersected (i.e., checks for the presence of ridge lines along gable roofs). After detecting the parts of the boundaries corresponding to the ridge lines the remaining boundaries of the sloping planar patches are further investigated. Next, horizontal planes are constructed by using the horizontal parts of the remaining boundaries. More specifically, height frequency of the boundaries is investigated to construct horizontal planes. The horizontal lines along the eaves of the sloping planar patches are acquired through the intersection between the constructed horizontal planes and corresponding planar patches. Then, the other remaining boundaries are regularized through Douglas-Peuker method and line fitting algorithms. After the refined lines are acquired by three different boundary regularization procedures, the proximity and collinearity in 2D space between the refined lines are investigated to figure out if the planar patches to which these lines belong are physically

connected through the vertical planes shared by them. The refined lines sharing the same vertical plane are recognized and utilized to derive an estimate of the vertical plane. Then, the lines are redefined based on the computed vertical plane. Finally, these lines are connected to construct a closed wire frame. Figure 12 displays the produced roof top wire frame through all the previous procedures. In addition, a 3D wire frame is generated using the average elevation of the ground around the buildings in Figure 13.

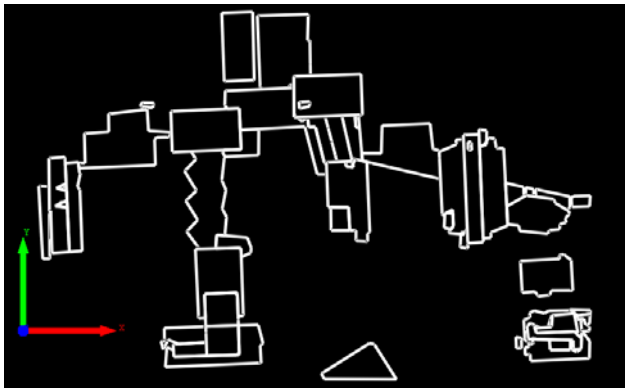

Figure 12. Refined rooftop boundaries.

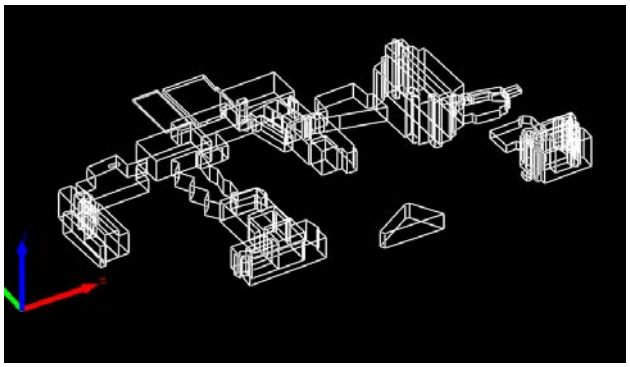

Figure 13. Constructed 3D wire frame

3. DISCUSSIONS

The performance of the proposed methodology has been visually evaluated by the projected DBM onto the orthophoto. Figure 14 shows the main buildings in the entire study area and their refined rooftop boundaries (shown as red lines) projected on the orthophoto. Most of roofs in the figure are reconstructed correctly in terms of completeness of the structural shape.

Detailed investigation of each roof is conducted by taking a closer look at Figure 15 and 16. Roof 1, 2, 4, 5, 6, and 7, which include orthogonal lines are reconstructed correctly in most parts. All the boundaries of roof 3, which are relevant to three different sloping planes, are well detected. Moreover, the non-orthogonal lines on roof 8 are reconstructed quite well. However, some of small details, which are enclosed by white solid circles, are lost on roof 2, 4, 5, and 6 due to the occlusion in the LiDAR data, inaccurate initial boundaries, and small structures on the roof.

Figure 14. Projected rooftop boundaries onto the orthophoto

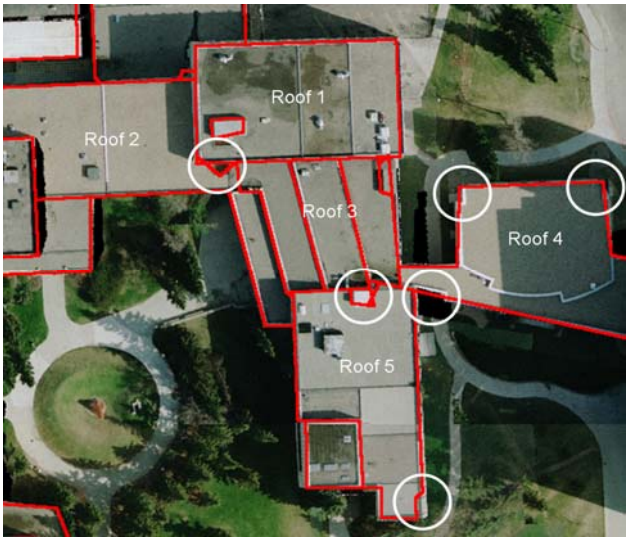

Figure 15. Boundaries of roof 1, 2, 3, 4, and 5 on orthophoto.

Figure 16. Boundaries of roof 6, 7, and 8 onto the orthophoto.

4. CONCLUSIONS

An automatic solution for DBM generation for complex structures from raw LiDAR data is introduced through four main procedures: ground/non-ground point separation; building hypothesis generation; segmentation of planar patches and intermediate boundary generation; and boundary refinement and 3D wire frame generation. First, a robust ground/non-ground point classification technique is proposed based on the novel idea of detecting points that produce occlusions. A building hypothesis generation procedure is devised based on the geometric characteristics of man-made structures. A segmentation procedure which simultaneously considers similarity attributes and proximity in the object space to derive robust and accurate solution was then performed. In the last step of the proposed methodology, several geometric constraints are applied to delineate the boundaries and to construct 3D wire frames for complex structures. The experimental results prove that the proposed methodology can provide a relatively accurate solution from raw LiDAR data. Moreover, it is proved that the limitation of the LiDAR data resolution causes deterioration of the accuracy of DBM as well as loss of details, especially for complex man-made structures. The limitations of the LiDAR data in the generation of DBM can be overcome by incorporating high resolution imagery into the procedures. More rich semantic information from high resolution imagery will help to improve the accuracy of the DBM and to detect edge details of buildings. Therefore, further research on the integration of LiDAR data and imagery will be investigated as future work.

ACKNOWLEDGEMENT

We would like to thank the GEOIDE (GEOmatics for Informed DEcisions) Network of Centers of Excellence of Canada (SII#43) and ETRI (Electronics and Telecommunications Research Institute) for their partial financial support of this research.

REFERENCES

Brenner, C., and Haala, N. (1998). Rapid acquisition of virtual reality city models from multiple data sources, *International Archives of Photogrammetry and Remote Sensing*, 32(5): 323-330.

Brunn, A., and U.Weidner, 1997. Extracting building from digital surface models, International Archives of Photogrammetry and Remote Sensing, 34(3-4): 27-34.

Ameri, B. , 2000. Automatic recognition and 3D reconstruction of buildings from digital imagery, *Deutsche Geodaetische Kommission*, Series C, No. 526.

Chang, Y., C. Kim, A. Kersting, and A. Habib, 2007. New approach for DTM generation from LiDAR data, *The 28th Asian Conference on Remote Sensing (ACRS)*, Kuala Lumpur , Malaysia, (Nov. 12-16, 2007).

Douglas, D.H., and T.K. Peucker, Algorithms for the reductions of the number of points required to represent a digitized line or its caricature, *The Canadian Cartographer* 10(2), pp. 112-122 (1973).

Filin, S., Pfeifer, N., 2006. Segmentation of airborne laser scanning data using a slope adaptive neighborhood. In: *ISPRS Journal of Photogrammetry & Remote Sensing*, 60, pp. 71–80.

Haala, N., Brenner, C., and Anders, K.-H. (1998). 3D urban GIS from laser altimeter and 2D map data, *International Archives of Photogrammetry and Remote Sensing*, 32(3/1): 339-346.

Habib, A., E. Kim, and C. Kim, 2007. New methodologies for true orthophoto generation, *Photogrammetric Engineering and Remote Sensing*, 73(1), pp. 25-36.

Habib, A., Y. Chang, D. Lee. Occlusion-Based Methodology for the Classification of LiDAR Data, *Photogrammetric Engineering & Remote Sensing* Submitted on January 25, 2008

Jarvis, R. A., 1977. Computing the shape hull of points in the plane, *Proceedings of IEEE Computer Society Conference Pattern Recognition and Image Process*, pp.231-261

Rottensteiner, F., and C. Briese, 2002. A new method for building extraction in urban areas from high resolution lidar data, *Proceedings of the ISPRS Commission III Symposium*, Graz, Austria, unpaginated CD-ROM.

Vosselman, G., and S. Dijkman, 2001. 3D building model reconstruction from point clouds and ground plans, *International Archives of Photogrammetry and Remote Sensing*, 34(3W4): 37-43.